Chapter 5

DEFLECTION ANGLE AND LENSING OBSERVABLES FOR THE ELLIS WORMHOLE

5.1 Introduction

Gravitational lensing by a massive compact lens is considered as an effective tool to study the signatures of peculiar astrophysical objects like extra solar planets, dark matter substructures, cosmological parameters (including dark energy), black hole etc. There could be strong and weak field effects on light deflection, hence on lensing observables. In any spherically symmetric gravity, one can define a photon sphere, which cannot be penetreted by ingoing light rays − they are captured right on the surface of that sphere. The weak field limit occurs when the light passes very far away from the lensing object, i.e., the closest approach to the lens is greater than the radius of the photon sphere giving a small deflection angle. The strong deflection limit occurs when light passes close to the surface of the photon sphere with larger bending angle and sometimes wind around the lens before reaching the observer giving more than one relativistics images. In the literature, many studies have been done on the gravitational lensing in weak field limit using analytical and numerical method. For instance, Rindler *et al* [1] used the analytical approach in weak deflection limit and confirmed the dependence of the parameters appearing in the metric. This approach was successfully implemented by other authors also [2]. Amore *et al* [3] studied both weak and strong limits simultaneously using a different analytical method but the results are not very accurate. Nonetheless, all these investigations have indeed provided us with a huge amount of information about the signatures of astrophysical objects.

One such exciting astrophysical object, which we discuss in this chapter, is a traversable wormhole. Wormholes are spacetime regions with two mouths connected by a throat. They are the solutions of the Einstein's equations of general relativity. Since the throat by definition is not supposed to be inside the event horizon and with no singularity inside, massive particles or photons pass from one side of the wormholes to the other. Morris and Thorne [4] have shown that the matter required for the feasiblity of wormholes must violate atleast some of the known energy conditions, the minimal violation being that of the Null Energy Condition (NEC), that is, wormhole matter must satisfy $p_r + \rho < 0$. The matter for $p_r + \rho < 0$ is known as *exotic matter* (Deatils of wormhole has been discussed in the introductory chapter). Lensing by stellar size wormholes is an attractive possibility and there is a lot of current interest among the scientific community about this possibility.

Work in the direction of lensing by wormholes has been initiated by Cramer *et al* [5]. Since then, gravitational lensing by various wormholes has been investigated [6]. Safanova *et al* [7] examined the lensing effects of negative masses on the light rays from point sources. Tsukamoto *et al* [8] studied the difference between black hole and wormhole by their Einstein-ring systems. Recently, Rahaman *et al* [9] pointed out that the galactic halos can support traversable wormholes. Observational lending signatures of the wormhole will not only establish the existence of wormhole but will also throw some light on the existence of exotic matter itself.

There exist numerous solutions of the Einstein minimally coupled scalar (EMS) field theory. We shall consider a particular massive wormhole solution of the EMS field theory, which is also known as Ellis II wormhole solution (*the* Ellis wormhole). Even though there exist other classes of EMS solutions, called EMS II-IV (III and IV are not considered here), EMS I (Ellis I) has received considerable attention . (See all the EMS I,II,III, IV solutions in [21,18]). For instance, gravitational lensing of the massless Ellis I wormhole geometry was studied by Dey and Sen [10], Abe [11] and Toki *et al* [12] in the weak gravitational field. Following Bozza [20], Nandi *et al* [13] worked out the lensing properties of the *singular* Ellis I wormhole solution in the strong deflection limit. (For related works, see: Perlick [14], Tejeiro and Larranga [15]). Study of light deflection by massless Ellis I wormhole done by Bhattacharya *et al* [2] has shown that only the proper radial distance l describes the two-way light deflection rather than the standard radial coordinate r_S. Nakajima and Asada [16] recently clarified the reason for having different forms of expression of deflection angle due to massless Ellis I wormhole. For light deflection in the Ellis wormhole, we adopt the PPN method developed by Keeton and Petters [17] for finding the gravitational lensing observables caused by compact objects, which allows one to test different theories of gravity. The purpose of this chapter is to theoretically examine how such lensing observables for the Ellis wormhole would differ from those of the Schwarzschild black hole.

The chapter is organised as follows. In Sec.5.2, we discuss about the line element of Ellis wormhole solution. In Sec.5.3, we outline the procedure of the Keeton-Petters method based on PPN appoach and obtain the Taylor series expansion of the deflection angle of light ray in terms of $\frac{M}{b}$. In the next Sec.5.4, we determine image position, magnification, time delay, weighted-centriod magnification and total magnification by obtaining its Taylor series expansion in terms of the dimensionless parameter ε that represents the angle substended by the gravitational radius normalised by the Einstein radius. We summarize the chapter in Sec.5.5.

5.2 Ellis wormhole

Ellis II wormhole (or simply *the* Ellis wormhole) is a soution of the EMS theory, which can be found in [21,18] among other two classes (I and III) of solutions. The action of the EMS is

$$\mathcal{A} = \int d^4x\sqrt{-g}\left[R - \varkappa g^{\mu\nu}\varphi_{,\mu}\varphi_{,\nu}\right] \tag{5.1}$$

and the field equations are given by

$$R_{\mu\nu} = \varkappa\varphi_{,\mu}\varphi_{,\nu} \tag{5.2}$$

$$\Box^2\varphi = 0 \tag{5.3}$$

where $\varkappa$ is a constant and φ is the massless scalar field and $\varkappa = -1$ represents the ghost scalar or exotic matter as it violates all energy conditions.

Here we present the Ellis wormhole in isotropic coordinates, which are obtained by solving the above two Eqs.(5.2) and (5.3). It is given by,

$$\begin{aligned} d\tau^2 &= -P(r)dt^2 + Q(r)\left[dr^2 + r^2\left(d\theta^2 + \sin^2\theta d\varphi^2\right)\right] \\ P(r) &= \exp\left[-2\pi\eta + 4\eta\tan^{-1}\left(\frac{r}{B}\right)\right] \\ Q(r) &= \left(1 + \frac{B^2}{r^2}\right)^2 \frac{1}{P(r)} \\ \phi(r) &= 2\lambda\tan^{-1}\left(\frac{r}{B}\right) \end{aligned} \tag{5.4}$$

where $2\lambda^2 = 1+\eta^2$ and η, B, λ are arbitrary constants. This solution has a conserved total energy $M = 2B\eta$. Nandi and Zhang [18] have pointed out that the Ellis solution represents a traversable wormhole of the Morris-Thorne type having a coordinate throat at

$$r_0^{\pm} = B\left[\eta \pm \sqrt{1+\eta^2}\right] \tag{5.5}$$

also at zero mass limit, viz., $\eta = 0$, the metric does not represents a massless wormhole. One interesting fact of this solution is that for $\eta^2 = -1$, or $\eta = \pm i$, the above solution can be converted to the well known Schwarzschild black hole solution in isotropic coordinates though this is neither trivial nor widely known as yet.

5.3 Deflection angle by Keeton-Petters Method

Before going through the bending angle and the lensing observables, we briefly outline the Keeton-Petters method [17]. It is a method based on the post-post-Newtonian (PPN) approach (the metric can be written as Taylor's series in $\frac{m}{r}$). To study the gravitational lensing by a compact deflector with mass m, Keeton and Petters introduced an analytical approach, where the whole lensing scenerio must satisfy the following assumptions:

[A1] The gravitational lens is compact, static and spherically symmetric with an asymptotically flat spacetime geometry sufficiently far from the lens. The spacetime is vacuum outside the lens and flat in abscence of the lens.

[**A2**] The observer and the source lie in the asymptotically flat regime of the spacetime.

[**A3**] The light ray's distance of closest approach r_0 and impact parameter b both lie well outside the gravitational radius $m = \frac{GM}{c^2}$, namely, $\frac{m}{r_0} \ll 1$and $\frac{m}{b} \ll 1$. The bending angle can then be expressed as a series expansion as follows in $\frac{m}{b}$:

$$\widehat{\alpha}(b) = A_1 \left(\frac{m}{b}\right) + A_2 \left(\frac{m}{b}\right)^2 + A_3 \left(\frac{m}{b}\right)^3 + O\left(\frac{m}{b}\right)^4. \tag{5.6}$$

The coefficients A_i are independent of $\frac{m}{b}$, but may include other fixed parameters of the spacetime. Since b and m are invariants of the light ray, Eq.(5.6) is independent of coordinates. Note that the subscript of A_i conveniently indicates that the component is affiliated with a term of order i in $\frac{m}{b}$.

We start with an isotropic form of a general spacetime metric given by

$$ds^2 = -A(r)dt^2 + B(r)\left\{dr^2 + r^2\left(d^2\theta + \sin^2\theta d\varphi^2\right)\right\}. \tag{5.7}$$

Now using the PPN formalism, we first express the coefficients of the metric (5.7) in a PPN series upto third order as follows

$$A(r) = 1 + 2\alpha_1\left(\frac{\phi}{c^2}\right) + 2\beta_1\left(\frac{\phi}{c^2}\right)^2 + \frac{3}{2}\delta_1\left(\frac{\phi}{c^2}\right)^3 + ..., \tag{5.8}$$

$$B(r) = 1 - 2\gamma_1\left(\frac{\phi}{c^2}\right) + \frac{3}{2}\xi_1\left(\frac{\phi}{c^2}\right)^2 - \frac{1}{2}\eta_1\left(\frac{\phi}{c^2}\right)^3 + ..., \tag{5.9}$$

where ϕ is the three-dimensional Newtonian potential with

$$\frac{\phi}{c^2} = -\frac{m}{r} \tag{5.10}$$

and α_1, β_1, δ_1, γ_1, ξ_1 and η_1 denote the Eddington-Robertson parameters and they are so chosen that the Schwarzschild metric has $\alpha_1 = \beta_1 = \delta_1 = \gamma_1 = \xi_1 = \eta_1 = 1$.

Finally the deflection angle is written in terms of the impact parameter b as,

$$\widehat{\alpha}(b) = A_1 \left(\frac{m}{b}\right) + A_2 \left(\frac{m}{b}\right)^2 + A_3 \left(\frac{m}{b}\right)^3 + O\left(\frac{m}{b}\right)^4, \tag{5.11}$$

where the coefficients in terms of Eddington-Robertson parameters can be found to be [17]

$$
\begin{aligned}
A_1 &= 2(\alpha_1+\gamma_1), && (5.12)\\
A_2 &= \left(2\alpha_1^2-\beta_1+2\alpha_1\gamma_1+\frac{3\xi_1}{4}\right)\pi, && (5.13)\\
A_3 &= \frac{1}{3}\left[70\alpha_1^3+90\alpha_1^2\gamma_1-36\beta_1\gamma_1-2\gamma_1^3+9\gamma_1\xi_1-60\alpha_1\beta_1\right.\\
&\quad \left.-18\alpha_1\delta_1^2-27\alpha_1\xi_1+3\eta_1+9\delta_1\right]. && (5.14)
\end{aligned}
$$

To apply this formalism to Ellis wormhole (5.4), we first express the metric functions into PPN series upto third order

$$
\begin{aligned}
P(r) &= 1-2\frac{M}{r}+2\left(\frac{M}{r}\right)^2+\frac{(1-8\eta^2)}{6\eta^2}\left(\frac{M}{r}\right)^3, && (5.15)\\
Q(r) &= 1+2\frac{M}{r}+\left(2+\frac{1}{2\eta^2}\right)\left(\frac{M}{r}\right)^2+\left(\frac{5+8\eta^2}{6\eta^2}\right)\left(\frac{M}{r}\right)^3. && (5.16)
\end{aligned}
$$

Then comparing Eqs.(5.8), (5.9), (5.15), (5.16), we get the following relations

$$
\alpha_1=1,\ \beta_1=1,\ \delta_1=-\frac{2}{3}\frac{(1-8\eta^2)}{6\eta^2},\ \gamma_1=1,\ \xi_1=\frac{2}{3}\left(2+\frac{1}{2\eta^2}\right),\ \eta_1=\frac{5+8\eta^2}{3\eta^2}\ . \tag{5.17}
$$

Thus from Eqs.(5.12-5.14) the coefficients in the expansion of the bending angle are

$$
A_1=4,\qquad A_2=\frac{\pi}{4}\frac{1+16\eta^2}{\eta^2},\qquad A_3=\frac{16}{3}\left(9+\frac{1}{\eta^2}\right), \tag{5.18}
$$

and our deflection angle with respect to the impact parameter b reads

$$
\alpha=4\left(\frac{M}{b}\right)+\frac{\pi}{4}\frac{1+16\eta^2}{\eta^2}\left(\frac{M}{b}\right)^2+\frac{16}{3}\left(9+\frac{1}{\eta^2}\right)\left(\frac{M}{b}\right)^3. \tag{5.19}
$$

Also we can arrive to Schwarzschild bending [17] upto order of M^3 just by putting $\eta^2=-1$, i.e., an imaginary η.

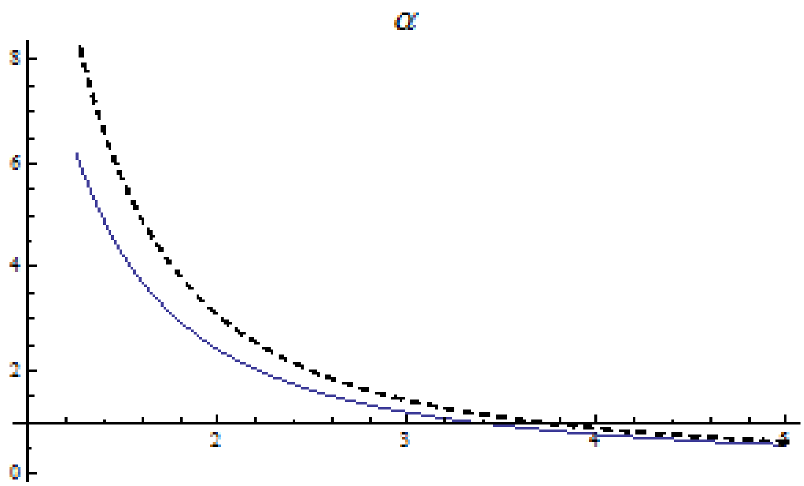

Fig. 5.1. Variation of deflection angle is shown with respect to the dimensionless impact parameter $\frac{b}{2M}$. Solid blue line gives the Schwarzschild bending ($\eta^2 = -1$), dashed line gives EMS class II solution (taking $\eta = 0.5$).

Next we calculate the image positions, magnifications and time delays of the primary and secondary lensed images using pertubative series solution of the lens equation.

5.4 Image position, Magnification and Time delay

We start with a general lens quation (For details, see [17]),

$$\tan \mathcal{B} = \tan \vartheta - D\left(\tan \vartheta + \tan\left(\widehat{\alpha} - \vartheta\right)\right), \tag{5.20}$$

where β and ϑ are angular position of source and image measured from the optic axis, $D = \frac{D_{ls}}{D_s}$, D_{ls} and D_s is the source-lens and source-observer distance respectively and $\widehat{\alpha}$ is the deflection angle.

We rescale the angular parameters as

$$\beta = \frac{\mathcal{B}}{\vartheta_E}, \ \theta = \frac{\vartheta}{\vartheta_E}.$$

i.e., both β and θ are the scaled angular positions of the source and image respectively. Here ϑ_E is the weak deflection angular Einstein radius,

$$\vartheta_E = \sqrt{\frac{4mD}{D_l}},$$

where D_l is the observer-lens distance, m is the gravtational radius of lens, $m = \frac{GM}{c^2}$ and M the physical mass.

According to the formalism given by Keeton-Petters method, solution of the lens equation (5.20) can be written as a series expansion of the form,

$$\theta = \theta_0 + \theta_1\varepsilon + \theta_2\varepsilon^2 + \mathcal{O}(\varepsilon)^3, \tag{5.21}$$

where θ_0 is the image position in the weak deflection limit and the coefficients θ_1 and θ_2 are the first and second order correction terms respectively, which should be determined. The dimensionless parameter ε represents the angle substended by the gravitational radius normalised by the Einstein radius. This quantity is taken as the small expansion parameter and is expressed as

$$\varepsilon = \frac{\vartheta_E}{4D}.$$

With the above substitution, the lens Eq.(5.20) becomes,

$$\begin{aligned} 0 \;=\; & D\left[-4\beta + 4\theta_0 - \frac{A_1}{\theta_0}\right]\varepsilon + \frac{D}{\theta_0^2}\left[-A_2 + \left(A_1 + 4\theta_0^2\right)\theta_1\right]\varepsilon^2 \\ & + \frac{D}{3\theta_0^3}\left[-A_1^3 - 3A_3 + 12A_1^2 D\theta_0^2 - A_1\left(56D^2\theta_0^4 + 3\theta_1^2 - 3\theta_0\theta_2\right)\right. \\ & \left. + 64D^2\theta_0^3\left(\theta_0^3 - \beta^3\right) + 6A_2\theta_1 + 12\theta_0^3\theta_2\right]\varepsilon^3 + O(\varepsilon)^4. \end{aligned} \tag{5.22}$$

To find the value of θ_i, we fix the source position β and solve the lens equation (5.22) term by term. The obtained solutions are as follows

$$\theta_0 = \frac{1}{2}\left(\beta + \sqrt{\beta^2 + 4}\right), \tag{5.23}$$

is the zeroth order term. The first order term leads to

$$\theta_1 = \frac{\pi}{4}\frac{16 + \dfrac{1}{\eta^2}}{2\left\{4 + \left(\beta + \sqrt{4 + \beta^2}\right)^2\right\}}, \tag{5.24}$$

and the second order term gives

$$\theta_2 = \frac{1}{3(\beta+\sqrt{4+\beta^2})\left\{4+(\beta+\sqrt{4+\beta^2})^2\right\}^3}\left[2\left\{16D_1(-3+4D_1)(\beta+\sqrt{4+\beta^2})^6\right.\right.$$
$$+2D_1^2(\beta+\sqrt{4+\beta^2})^8+4\left\{-256(-1+D_1^2)-\frac{3}{16}\pi^2(16+\frac{1}{\eta^2})^2\right.$$
$$\left.+64\left(9+\frac{1}{\eta^2}\right)\right\}+(\beta+\sqrt{4+\beta^2})^2\left\{256(-2+D_1)(-1+D_1)\right.$$
$$\left.+128\left(9+\frac{1}{\eta^2}\right)-\frac{3}{8}\pi^2(16+\frac{1}{\eta^2})^2\right\}+\frac{1}{\eta^2}\left[16(\beta+\sqrt{4+\beta^2})^4\right.$$
$$\left.\left.\left.\left\{1+\left(13-24D_1+22D_1^2\right)\eta^2\right\}\right]\right\}\right]. \tag{5.25}$$

Thus the image position θ is given by Eqs.(5.21, 5.23, 5.24, 5.25). It should be noted that for each β any source is imaged twice i.e., for $\beta > 0$ we find the positive parity image θ^+ (primary) and for $\beta < 0$ negative parity θ^- (secondary) and both images lies on the opposite sides of the lens such that $\theta^-(\beta) = \theta^+(-\beta)$. For a particular value $\beta = 0$, we obtain the position of the Einstein ring.

We next study another important source of information i.e., the magnification of the images. The magnification μ of the lensed image is given by,

$$\mu = \left|\frac{\sin\beta}{\sin\theta}\frac{d\beta}{d\theta}\right|^{-1},$$

in which $\mu_t = \left(\frac{\sin\beta}{\sin\theta}\right)^{-1}$ is the tangential magnification and $\mu_r = \left(\frac{d\beta}{d\theta}\right)^{-1}$ is the radial magnification. We now express μ with respect to the order parameter ε and write the series

$$\mu = \mu_0 + \mu_1\varepsilon + \mu_2\varepsilon^2 + \mathcal{O}(\varepsilon)^3, \tag{5.26}$$

where

$$\mu_0 = \frac{\left(\beta+\sqrt{\beta^2+4}\right)^4}{-16+\left(\beta+\sqrt{\beta^2+4}\right)^4}, \tag{5.27}$$

$$\mu_1 = -\frac{\pi\left(\beta+\sqrt{\beta^2+4}\right)^3\left(16+\frac{1}{\eta^2}\right)}{2\left\{4+\left(\beta+\sqrt{\beta^2+4}\right)^2\right\}^3}, \tag{5.28}$$

$$\begin{aligned}\mu_2 = {} & \frac{-\left(\beta+\sqrt{\beta^2+4}\right)}{3\beta\left\{4+\left(\beta+\sqrt{\beta^2+4}\right)^2\right\}^5}\left[-4096D_1^2-4D_1^2\left(\beta+\sqrt{\beta^2+4}\right)^8\right. \\ & +64\left(\beta+\sqrt{\beta^2+4}\right)^6\left(13+12D_1-18D_1^2+\frac{1}{\eta^2}\right) \\ & -2\left(\beta+\sqrt{\beta^2+4}\right)^4\left\{256\left(-4-12D_1+17D_1^2\right)-256\left(9+\frac{1}{\eta^2}\right)\right. \\ & \left.\left.+\frac{9}{8}\pi^2\left(16+\frac{1}{\eta^2}\right)^2\right\}-1024\left(\beta+\sqrt{\beta^2+4}\right)^2\left(13+12D_1-18D_1^2+\frac{1}{\eta^2}\right)\right].\end{aligned} \tag{5.29}$$

Thus the magnification is given by Eqs.(5.26, 5.27, 5.28 and 5.29). The above coefficients also have the positive parity and negative parity for corresponding values of β, so that $\mu^+(-\beta) = \mu^-(\beta)$.

In case, the position of the primary and secondary images are close together to be extricable, total magnificaion and magnification-weighted centroid plays a vital role to study the gravitational lensing. Using our result we find the total magnification as,

$$\begin{aligned}\mu_{tot} = {} & \left|\mu^+\right|+\left|\mu^-\right| = \frac{2+\beta^2}{\beta\sqrt{4+\beta^2}}\times\frac{1}{192\beta\eta^4\left(4+\beta^2\right)^{\frac{5}{2}}}\times\left[9\left(\pi+16\pi\eta^2\right)^2\right. \\ & \left.+1024\eta^2\left(4+\beta^2\right)\left\{-1+\eta^2\left(-13-12D_1+D_1^2\left(18+\beta^2\right)\right)\right\}\right]\varepsilon^2\end{aligned} \tag{5.30}$$

and magnification-weighted centroid as,

$$\Theta_{cent} = \frac{\theta^+\left|\mu^+\right|+\theta^-\left|\mu^-\right|}{\left|\mu^+\right|-\left|\mu^-\right|}, \tag{5.31}$$

which can be written in terms of the expansion parameter ε as,

$$\Theta_{cent} = \Theta_0 + \Theta_1\varepsilon + \Theta_2\varepsilon^2, \tag{5.32}$$

where

$$\Theta_0 = \frac{\theta_0^+\mu_0^+ + \theta_0^-\mu_0^-}{\mu_0^+ - \mu_0^-}, \tag{5.33}$$

$$\Theta_1 = \frac{\theta_1^-\mu_0^- + \theta_0^+\mu_1^+ + \theta_0^-\mu_1^- + \theta_1^+\mu_0^+}{\mu_0^+ - \mu_0^-}, \tag{5.34}$$

$$\Theta_2 = \frac{(\theta_0^+ + \theta_0^-)(\mu_0^+\mu_2^- - \mu_0^-\mu_2^+) + (\mu_0^+ - \mu_0^-)\left[\mu_1^+(\theta_1^+ + \theta_1^-) + \theta_2^+\mu_0^+ + \theta_2^-\mu_0^-\right]}{\left(\mu_0^+ - \mu_0^-\right)^2}. \tag{5.35}$$

Since the expression for Θ_{cent} is too large to write, we skip writing the expression but the calculation is straight forward and the reader can simply put the above results and can find out the expression. Here $+$ denotes the positive parity of image and $-$ denotes the negative parity.

After studying position and magnification of lensed images, we are now to compute the time delays the light suffers while coming to us from both the images. In series expansion, with respect to the order parameter ε time delay $\widehat{\tau}$ is given by

$$\widehat{\tau} = \widehat{\tau}_0 + \widehat{\tau}_1\varepsilon + \mathcal{O}(\varepsilon^2)\ , \tag{5.36}$$

where,

$$\widehat{\tau}_0 = \frac{1}{2}\left\{1 + \beta^2 - \frac{1}{4}\left(\beta + \sqrt{4+\beta^2}\right)^2 - \ln\left[\frac{d_{ol}\vartheta_E^2\left(\beta + \sqrt{4+\beta^2}\right)^2}{16 d_{ls}}\right]\right\}, \tag{5.37}$$

and

$$\widehat{\tau}_1 = \frac{\pi\left(16 + \frac{1}{\eta^2}\right)}{8\left(\beta + \sqrt{4+\beta^2}\right)}. \tag{5.38}$$

The final expression for time delay is given by, Eqs.(5.36, 5.37 and 5.38).

To explore the physical content, we proceed to the various lensing observables for Ellis wormhole graphically. For this, we assme that at the center of our Milky Way galaxy (lens), there is the positive mouth of the Ellis wormhole with mass $M = m\beta$

instead of the widely speculated supermassive black hole. So we take $M = 4.31 \times 10^6 M_\odot$ and the lens-observer distance $D_l = 8.33$ kpc. For the lens-source distance, following [19], we have taken $D_{ls} = 0.005 \times D_l$. Furthermore, we consider that the lens is situated at half way between the source and the observer i.e. $\dfrac{D_{ls}}{D_s} = \dfrac{1}{2}$. Diagram for the image position, magnification, total magnification, magnification-weighted centroid and the time delay of Ellis wormhole is plotted in Figs.5.2-5.6 respectively with respect to the source position β. Solid line corresponds to $\eta^2 = -1$, and dot-dashed line corresponds to $\eta = 0.0005$ respectively.

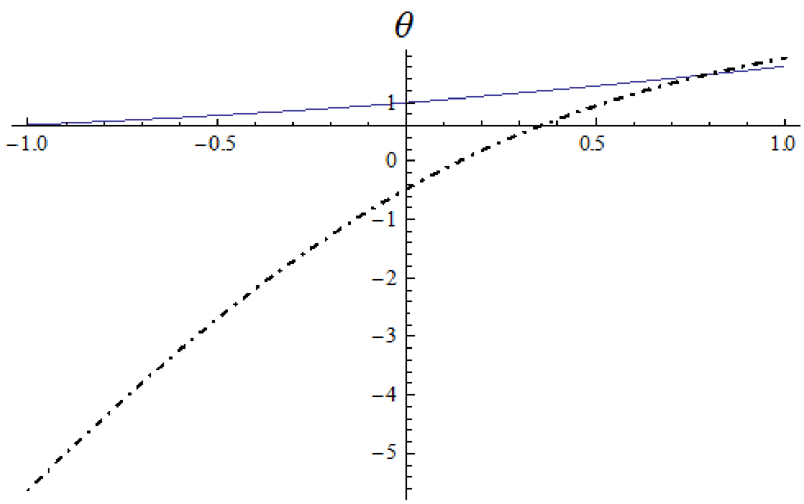

Fig. 5.2

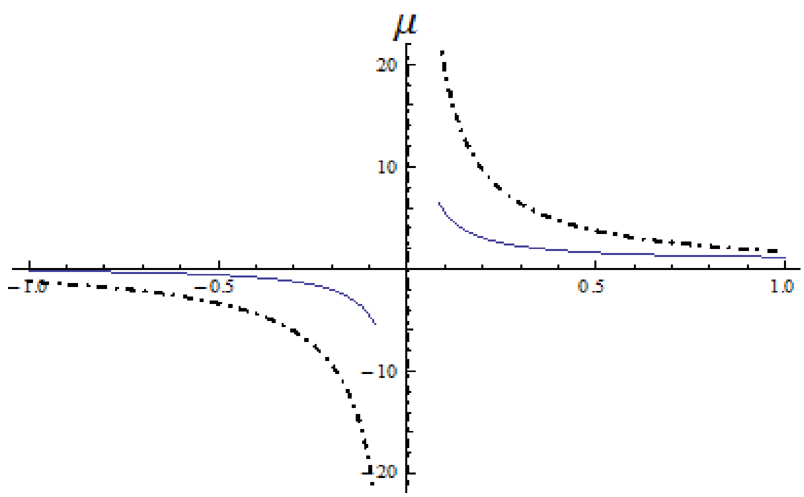

Fig. 5.3

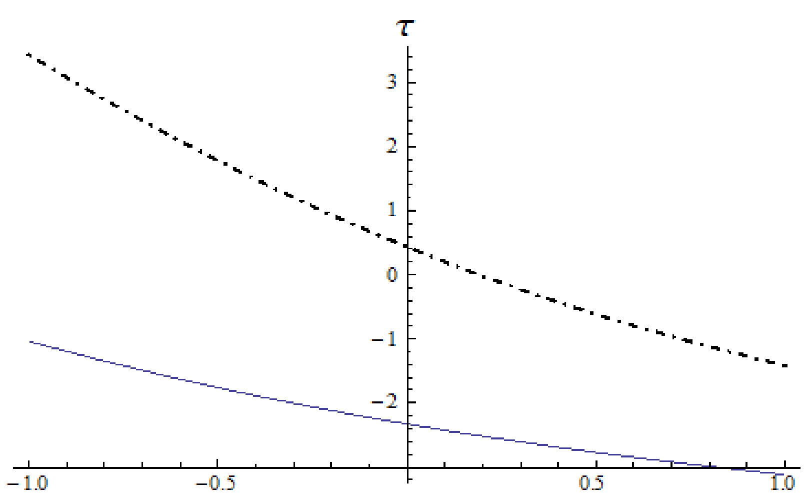

Fig. 5.4

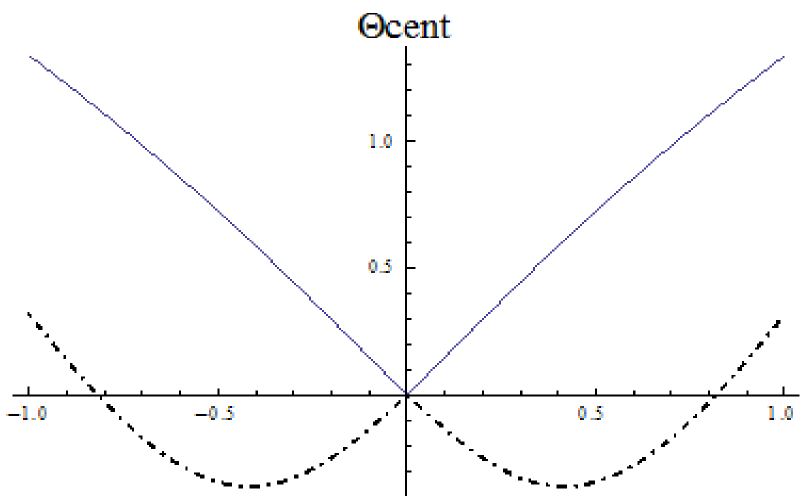

Fig. 5.5

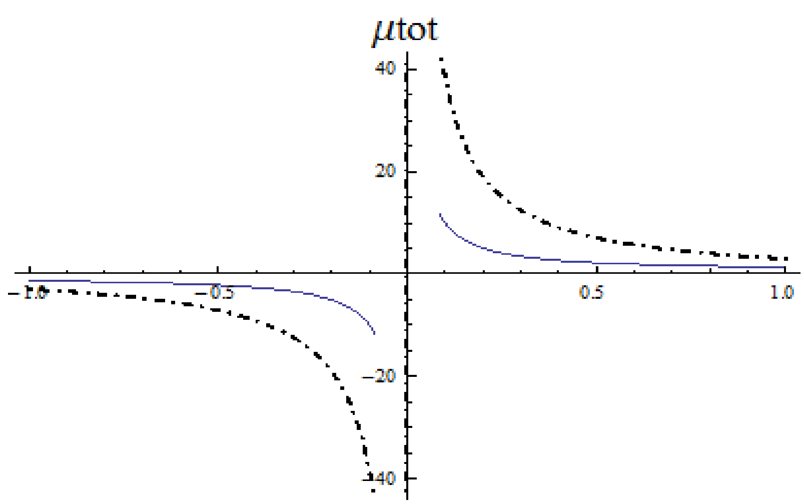

Fig. 5.6

Fig.5.2, Fig.5.3, Fig.5.4, Fig.5.5 and Fig.5.6 shows the variations of image position (θ), magnification (μ), time delay (τ), magnification-weighted centroid (Θ_{cent}) and total magnification (μ_{tot}) respectively with respect to the source position β. $\eta^2 = -1$ represents the solid line (Schwarzschild) and $\eta = 0.0005$ represents the dot-dashed line.

5.5 Conclusion

We obtained the deflection angle of light ray in weak deflection limit for EMS class II wormhole solution. Unfortunately, this solution hasn't received a lot of attention in the literature. PPN approach of Keeton and Petters is used to obtain the deflection angle, position, magnification, magnification weighted centroid, total magnifiation and time delay of the relativistic images, where the lensing observables are expressed in series with respect to the order parameter ε. Bending angle of the wormhole solution is compared with the Schwarzschild bending which shows that the light bending by Ellis wormhole is quite distinguishable from that by the Schwarzschild black hole ($\eta^2 = -1$). Also lensing observables are represented graphically with respect to the source position β, which show considerable deviation from those in the Schwarzschild black hole. From all the obtained results what we can say that, these deviations could help distinguish wormholes from black holes by means of gravitational lensing.

5.6 References

[1] W. Rindler, M. Ishak, Phys. Rev. D **76** 043006 (2007).

[2] M. Ishak, W. Rindler, J. Dossett, J. Moldenhauer and C. Allison, Mon. Not. Roy. Astron. Soc. **388**, 1279 (2008); M. Ishak, W. Rindler and J. Dosset, Mon. Not. Roy. Astron. Soc. **403**, 2152 (2010); M. Ishak and W. Rindler, Gen. Rel. Grav. **42**, 2247 (2010); A. Bhattacharya, R. Isaev M. Scalia, C. Cattani and Kamal K. Nandi, JCAP **09** (2010) 04; A. Bhattacharya and A. A. Potapov, Mod. Phys. lett. A **25**, 2399 (2010); A. Bhattacharya, G. M. Garipova, Ettore Lassera, A. Bhadra, Kamal K. Nandi, JCAP **02** (2011) 28.

[3] P. Amore and S. A. Diaz, Phys. Rev. D **73**, 083004 (2006).

[4] M.S. Morris and K.S. Thorne, Am. J. Phys. **56**, 395 (1988).

[5] J.G. Cramer, R.L. Forward, M.S. Morris, M. Visser, G. Benford, and G.A. Landis, Phys. Rev. D **51**, 3117 (1995).

[6] M. Safonova, D. F. Torres and G. E. Romero, Mod. Phys. Lett. A **16**, 153 (2001); E. Eiroa, G. E. Romero and D. F. Torres, Mod. Phys. Lett. A **16**, 973 (2001); M. Safonova and D. F. Torres, Mod. Phys. Lett. A **17**,

1685 (2002); K. K. Nandi, Y. Z. Zhang and A. V. Zakharov, Phys. Rev. D **74**, 024020 (2006); F. Rahaman, M. Kalam and S. Chakraborty, Chin. J. Phys. **45**, 518 (2007).

[7] M. Safonova, D.F. Torres, and G.E. Romero, Phys. Rev. D **65**, 023001 (2002).

[8] Naoki Tsukamoto, Tomohiro Harada, Kohji Yajima, Phys. Rev. D **86**, 104062 (2012).

[9] F. Rahaman, P.K.F. Kuhfittig, S. Ray and N. Islam, Eur. Phys. J. C **74**, 2750 (2014).

[10] T. K. Dey and S. Sen, Mod. Phys. Lett. A **23**, 953 (2008).

[11] F. Abe, Astrophys. J. **725**, 787 (2010).

[12] Y. Toki, T. Kitamura, H. Asada and F. Abe, Astrophys. J. **740**, 121 (2011).

[13] K. K. Nandi, Y. Z. Zhang and A. V. Zakharov, Phys. Rev. D **74**, 024020 (2006).

[14] V. Perlick, Phys. Rev. D **69**, 064017 (2004).

[15] J. M. Tejeiro and E. A. Larranaga, Rom. J. Phys. **57**, 736 (2012).

[16] K. Nakajima and H. Asada, Phys. Rev. D **85**, 107501 (2012).

[17] C. R. Keeton and Petters, Phys. Rev. D **72** 104006 (2005), Phys. Rev. **D 73** 044024 (2006) and Phys. Rev. **D 73** 104032 (2006).

[18] K. K. Nandi and Y. Z. Zhang, Phys.Rev. D **70**, 044040 (2004).

[19] K. S. Virbhadra, Phys. Rev. D **79**, 083004, (2009).

[20] V. Bozza, Phys. Rev. D **66**, 103001 (2002).

[21] H.G. Ellis, J. Math. Phys. **14**, 104 (1973); *Errata*: J. Math. Phys. **15**, 520 (1974).